

THE USE AND PREDICTIVE CAPABILITY OF CFD FOR FULLY DEVELOPED NATURAL FIRES IN LARGE COMPARTMENTS

George N. Koutlas*

*CORUS Research Development & Technology, Swinden Technology Centre
Moorgate Road, S60 3AR, Rotherham, UK
e-mail: george.koutlas@corusgroup.com

Key words: Fire Modelling, Fire Spread, Fire Growth, Smoke Movement, FDS Simulation

Abstract. *The purpose of the present study is to explore and validate the efficiency and accuracy of the predictive capability of CFD models for fully developed natural fires in large compartments. The FDS CFD software was used to simulate three large-scale fire tests. The fire tests (nine in total) had been carried out in 1993 at Cardington UK, in collaboration with BRE/FRS and CORUS (British Steel at that time). The main parameters of the three chosen large-scale fire tests are the compartment's dimensions, the fire load, the ventilation opening, and the ignition type. The duration of the fire tests, starting from the ignition until the extinction of the fire, was between 70-120 min and the fire source was wooden cribs. The simulations were in full time and full scale. The FDS model solves numerically the well known Navier-Stokes equations with emphasis on smoke and heat transport from fires. It uses a mixture fraction combustion model assuming that combustion is mixing controlled, and that the reaction of fuel and oxygen is infinitely fast. Turbulence is treated by means of the Smagorinsky form of Large Eddy Simulation, while thermal radiation is computed using a finite volume technique. Despite the assumptions made and the complex phenomena involved, the correlation between the computational and experimental results was in very good agreement. The fire spread was modelled accurately and the difference for the peak temperatures was 5%-20%. However the results are sensitive to some input parameters and so each fire scenario should be treated individually for a robust and accurate solution.*

1 INTRODUCTION

The idea that the dynamics of a fire might be studied numerically dates back to the beginning of the computer age. Indeed, the fundamental conservation equations governing fluid dynamics, heat transfer, and combustion were first written down over a century ago. Despite this, practical mathematical models of fire (as distinct from controlled combustion) are relatively recent due to the inherent complexity of the problem.

The difficulties revolve around three issues: First, there are an enormous number of possible fire scenarios to be considered due to their accidental nature. Second, the physical insight and computing power required to perform all the necessary calculations for most fire scenarios are limited. Any fundamentally based study of fires embraces nearly all the effects found in subsonic chemically reacting flows. Fluid dynamics, combustion, kinetics, radiation, and in many cases multi-phase flow effects are linked together to provide an extremely complex physical and chemical phenomenon. Finally, the "fuel" in most fires was never intended as such. Thus, the mathematical models and the data needed to characterise the degradation of the condensed phase materials that supply the fuel may not be available. Indeed, the mathematical modelling of the physical and chemical transformations of real materials as they burn is still in its infancy.

Mathematical modelling of fire is still young and it is a rapidly developing area of computational fluid dynamics. The complexity of the phenomenon makes it extremely challenging from the mathematical point of view. The underlying fluid dynamics, turbulence, and combustion problems have not yet been fully resolved and represent significant challenges themselves. Incorporation of all these processes into a unified computational model is even more formidable task.

Mathematical modelling of fires started from semi-empirical and analytical models¹⁻³. Their evolution then led to the development of zone models, which formed the first generation of computer fire models. The development of CFD modelling made it possible to model fire phenomena from first principles via solution of the basic conservation equations. This approach is known in fire research as field or CFD modelling. It has shown success in application to various fire safety problems and its role to fire research is steadily increasing as the models become more sophisticated and validation studies make them more reliable. The CFD approach is considered to be fundamental to the future development of fire models, which can provide the basis for the development of performance-based fire safety regulations.

The present study aims to explore and validate the efficiency and accuracy of the predictive capability of CFD for fully developed natural fires in large compartments. The Fire Dynamics Simulator (FDS) software from NIST was used to simulate three large-scale fire tests.

The current paper is divided into four main sections. In the first one, some details about the concept of the large-scale fire tests experiments are given. The second section deals with the main features of the FDS software while a few more details are given where necessary. In section three, a description and details about the way the simulations were set up and the main data used are given. Finally, in the last section, detailed results and comparisons are given, including explanations and a short discussion for the uncertainties and the assumptions made.

2 EXPERIMENTAL DETAILS – CONCEPT OF THE EXPERIMENTS

Corus - Swinden Technology Centre (British Steel at that time), in collaboration with the Building Research Establishment, Fire Research Station, have constructed a series of nine fire tests to simulate the behaviour of natural fires in large scale compartments. The tests were carried out in a purpose built compartment in the BRE Cardington Laboratory. The programme sponsored by the UK Department of Environment and Corus.

The main aim was to collect information on gas temperatures and temperature-time profiles for short lengths of protected and unprotected steel beam and column section, so that equivalent times of fire exposure could be deducted for different parameters. A secondary aim was to provide additional data of interest to modellers.

The external dimensions of the compartment were 23.12 m long, 6.12 m wide, and 3.07 m high, respectively. It represented a "slice" through a much larger compartment of 46 m deep and of infinite width. Its size and shape represented a large open plan office. Apart from Test 7, these dimensions corresponded approximately to a depth to width ratio of 4:1 and a depth to height ratio of 8:1. The ventilation opening was in one of the 6x3 m walls. There were no other ventilation openings. A general view of the structure is shown in Figure 1.

The floor comprised a nominal 100 mm thick layer of normal weight concrete with a 125 mm deep layer of "Chelford" 50 grade dry silica sand. The walls and roof consisted of a single layer of lightweight concrete blocks 440x215x215 mm and reinforced autoclaved aerated concrete slabs 6x0.7x0.2 m thick, respectively. Both walls and roof were lined with two 25 mm thick layers of ceramic fibre blanket, fixed with stainless steel pins. This assembly was further lined (for Test 8 only) with two 12.7 mm thick layers of Fireline glass fibre reinforced plasterboard. The relevant dimensions of the compartment are given in Table 1.

	External Dimensions (mm)		Internal Dimensions (mm)	
	Tests 1-6 and 9	Length	23.120	Length
Width		6.125	Width	5.595
Height		3.075	Height	2.750
Test 7	Length	5.860	Length	5.595
	Width	6.125	Width	5.595
	Height	3.075	Height	2.750
Test 8	Length	23.120	Length	22.780
	Width	6.125	Width	5.465
	Height	3.075	Height	2.680

Table 1: Dimensions of the compartment

The ventilation opening was in the front wall. This varied from 100% of the front wall area down to 12.5%, as shown in Figure 2. The opening was blocked with 50mm thick lightweight aerated concrete blocks and lined on the inside with two 25 mm thick layers of ceramic fibre blanket. Special care was taken for the moisture content control of the construction. Details of the relevant physical properties for each material are given in Table 2.

Structure	Materials	Density (kg/m ³)	Specific Heat [kJ/(kg K)]	Thermal conductivity [W/(m K)]
Walls	Lightweight concrete blocks	1375	0.753	0.42
Roof	Autoclaved aerated concrete	450	1.050	0.16
Floor	Fluid Sand	1750	0.800	1.0
Lining 1	Ceramic fibre	128	1.130	0.02
Lining 2	Fireline plasterboard	9 (kg/m ²)	1.250	0.24

Table 2: Ambient temperature properties of the materials used in the compartment

Figure 3 shows the detailed layout of the 33 (one meter square) cribs, distributed to provide a uniform fire load density. In the reduced size compartment (Test 7) nine cribs were used. Each crib was constructed using 1 m lengths of 50x50 mm Western Hemlock softwood (Figure 4). The moisture content was reduced to within the range 8-10% by weight. 155 sticks placed in 15 layers and 75 sticks in 7 layers were used, for a fire load density of 40 kg/m² and 20 kg/m² of floor area, respectively. On average, a 1 m length of softwood weighed 1 kg. The fires were ignited at the rear of the compartment (crib line 1) except for Test 7 and 9.

For the purpose of determining values of time equivalent, six short lengths I-section beams and columns were used. There were nominally 1 m long, with dimensions of 254x146 mm x 43 kg/m and 203x203 mm x 52 kg/m for the universal beams and columns, respectively. The sections were fixed to the underside of the insulated ceiling (Figure 5 and 6). Three of the beams and three of the columns were fire protected. For the Test 1 and 2 Vicuclad Grade 900 was used. However, as a result of the duration and severity of the fire the higher specification Vicuclad Grade 1050 was used for the rest of the tests.

Different parameters, like the mass-loss rate of fuel, combustion gas concentrations, velocity of inflowing air/outflowing gases, radiation intensity etc., were recorded during the experiments. Atmosphere temperature data were recorded in different positions, both inside and outside the compartment. There were temperature probes in the wall linings as well as in the steel members. The position of most the measurement probes is shown in Figure 5 - 7. The entire test programme^{4, 5} is summarised in Table 3.

	Test 1	Test 2	Test 3	Test 4	Test 5	Test 6	Test 7	Test 8	Test 9
Fire load density	40	20	20	40	20	20	20	20.6	20
% Ventilation	100	100	50	50	25	12.5	25	100	100
Compartment size	Full size	Full size	Full size	Full size	Full size	Full size	¼ size	Full size	Full size
Walls and ceiling lining	A	A	A	A	A	A	A	B	A
Crib ignition	C	C	C	C	C	C	D	C	D

A= ceramic fibre, B=plasterboard, C=growing, D=simultaneous

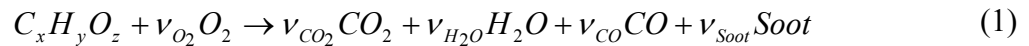
Table 3: Chosen parameters for the test programme

3 NUMERICAL PROCEDURE

The FDS version 4.0 software was used to simulate the three large-scale fire tests^{6,7}. FDS is a CFD model of fire-driven fluid flow. It was developed and is currently maintained by the Fire Research Division in the Building and Fire Research Laboratory (BFRL), at the National Institute of Standards and Technology (NIST).

FDS solves numerically a form of the Navier-Stokes equations⁸ appropriate for low-speed and thermally-driven flows, with an emphasis on smoke and heat transport from fires. The core algorithm is an explicit predictor-corrector scheme with second order accuracy in space and time. Turbulence is treated by means of the Smagorinsky form of Large Eddy Simulation (LES). It is possible to perform a Direct Numerical Simulation (DNS) if the underlying numerical grid is fine enough.

For most applications, FDS uses a mixture fraction combustion model. The mixture fraction is a conserved scalar quantity that is defined as the fraction of gas at a given point in the flow field that originated as fuel. The model assumes that combustion is mixing-controlled and that the reaction of fuel and oxygen is infinitely fast. The mass fractions of all the major reactants and products can be derived from the mixture fraction by means of "state relations". It is assumed that a single hydrocarbon fuel is being burned, with constant yields of CO and soot:



where, ν_i , with $i = O_2, CO_2, H_2O, CO,$ and $Soot$, are the stoichiometric coefficients of $O_2, CO_2, H_2O, CO,$ and soot, respectively. It is assumed that the CO and soot are created at the flame and transported with the combustion products. No growth, oxidation or after burning is assumed. The stoichiometric coefficients for $O_2, CO_2,$ and H_2O are adjusted to account for the production of CO and soot at the start of a calculation. The actual stoichiometric coefficients used in the calculations are:

$$\begin{aligned} \nu_{O_2} &= \left(x - \frac{M_f}{2M_{CO}} y_{CO} - \frac{M_f}{M_C} y_s \right) + \frac{y}{4} - \frac{z}{2} \\ \nu_{CO_2} &= x - \frac{M_f}{M_{CO}} y_{CO} - \frac{M_f}{M_C} y_s \\ \nu_{H_2O} &= \frac{y}{2} \\ \nu_{CO} &= \frac{M_f}{M_{CO}} y_{CO} \\ \nu_{Soot} &= \frac{M_f}{M_C} y_s \end{aligned} \quad (2)$$

where, y_{CO} is the mass fraction of fuel converted into carbon monoxide, y_s is the mass fraction of fuel converted into smoke particulate, and M_i , with $i = f, CO,$ and C , are the

molecular weights of fuel, CO, and C, respectively. The parameter y_s has a given value, usually 0.01, and it applies to the net production of the smoke particulate from the fire. The parameter y_{CO} is linked to the y_s and calculated automatically from the expression:

$$y_{CO} = \frac{12x}{M_f \nu_f} 0.0014 + 0.37y_s \quad (3)$$

where, x is the number of the carbon atoms in the fuel molecule, M_f is the molecular weight of the fuel, and ν_f is the stoichiometric coefficient of the fuel. Note that this correlation refers to well-ventilated fires. The yield of CO and soot in under-ventilated fires is still a subject of active research. The heat of combustion is slightly modified due to the presence of soot and CO, and is calculated from the expression:

$$\Delta H \approx \frac{\nu_{O_2} M_{O_2}}{\nu_f M_f} \Delta H_{O_2} \quad (4)$$

where, ΔH_{O_2} is the energy per unit mass of oxygen.

On coarse grids, the fire is not resolved adequately and as a result the heat release rate and flame height can be underestimated. A way to remedy the problem is by choosing a different value of the mixture fraction when defining the flame sheet. The program uses a routine that redefines the stoichiometric value of the mixture fraction according to:

$$\frac{Z_{f,eff}}{Z_f} = \min\left(1, C \frac{D^*}{\delta x}\right) \quad (5)$$

where, Z_f is the ideal stoichiometric value of the mixture fraction, C is an empirical constant, D^* is a characteristic fire diameter, and δx is the nominal size of a grid cell. The quantity $D^*/\delta x$ can be thought of as the number of computational cells spanning the characteristic diameter of the fire. The more cells spanning the fire, the better the resolution of the calculation.

Radiative heat transfer is included in the model via the solution of the radiation transport equation for a non-scattering grey gas. In a limited number of cases, a wide band model can be used in place of the grey gas model. The radiation equation is solved using a technique similar to a finite volume method for convective transport. Using approximately 100 discrete angles, the finite volume solver requires about 15 % of the total CPU time of a calculation.

FDS approximates the governing equations on one or more rectilinear grids. The rectangular obstructions, prescribed by the user, are forced to conform with the numerical grid. This can be a limitation in some situations where certain geometric features do not conform to the rectangular grid, although most building components do.

All solid surfaces are assigned thermal boundary conditions plus information about the burning behaviour of the material. The material properties can be stored in a separate database file and invoked by name. Heat and mass transfer to and from solid surfaces is handled with empirical correlations, unless the DNS model is used.

The model was originally designed to analyse industrial-scale fires. It can be used reliably

when the heat release rate of the fire is specified and the transport of heat and exhaust products is the principal aim of the simulation. In these cases, the model predicts flow velocities and temperatures to an accuracy within 5% to 20% of experimental measurements, depending on the resolution of the numerical grid. However, for fire scenarios where the heat release rate is predicted rather than prescribed, the uncertainty of the model is higher. That is because the properties of real materials and real fuels are often unknown or difficult to obtain; the physical processes of combustion, radiation, and solid phase heat transfer are more complicated than their mathematical representations in FDS; finally, the results of calculations are sensitive to both the numerical and physical parameters. Current research is aimed at improving this situation, but it is safe to say that modelling fire growth and spread will always require a higher level of user skill and judgment than that required for modelling the transport of smoke and heat from prescribed fires.

4 PROBLEM SET-UP

In the present study three of the large-scale fire test are presented Test 1, Test 2, and Test 3, respectively. Test 1 was simulated twice with few changes in the input file. The main and most important parameters used for the simulations are given below. Wherever is necessary a few more details are given.

4.1 Numerical grid and geometry

The geometry for Test 1 and Test 2 is the same, so a common approach was used. The computational geometry was split in two domains. The first main domain was the inside of the compartment while the second one was the outside. Because of the particular layout of the compartment, there was no extra benefit by splitting this area into more domains. A non-uniform grid was used, while there were slight differences to the stretch-grid factors, in order to adapt to the differences of the wood crib geometry in the two cases.

Test 7 was split in three domains. One domain was the inside of the compartment, while the outside was split into two. The outside domain in Test 7 differs from the one in Test 1 and 2, because some extra thermocouples were added there, to measure the fire plume temperatures. This new geometry was fully simulated but no further details are given here. The number of grid cells used for Test 1 and 2 were about 250000 each, while for Test 7 were about 150000. The meshes used were considered fine enough for that scale of simulations.

For a more accurate representation of the real geometry, both the protected and unprotected steel members were modelled and included in the computational geometry, despite the fact that there was no way to have a reliable calculation of the steel temperatures with the present FDS version. Furthermore, the wood cribs were modelled as "thick layers" rather than square boxes. However, there was no detailed study for the "real efficiency" of this approach.

Figure 8 shows the computational geometry for Test 1 and 7. All the thermocouple and pressure probes were included in the input file according to the information given. Some of them may be recognised as black dots in Figure 8.

4.2 Models and input data used

Temperature-dependant properties were used wherever they were available. The values are given in Table 4 and 5. The ambient temperature assumed to be, $T_{amb}=20\text{ }^{\circ}\text{C}$.

Structure	Materials	Temperature [$^{\circ}\text{C}$]	Thermal conductivity [W/(m K)]	Specific Heat [kJ/(kg K)]	Density [kg/m ³]
Walls	Ceramic fibre blanket	T=20	0.02	1.13	128.0
		T=400	0.07		
T=600		0.12			
Ceiling		T=800	0.16		
		T=1000	0.27		
		T=1200	0.34		
Steel members	Vicuclad	T=20	0.14	1.25	405.0
		T=200	0.16		
		T=400	0.19		
		T=600	0.22		
		T=700	0.24		
Wood Crib	Western Hemlock softwood	T=20	0.13	1.2	460.0
		T=500	0.29	3.0	

Table 4: Thermophysical properties for the structural materials and wood

Material	Temperature [$^{\circ}\text{C}$]	Thermal conductivity [W/(m K)]	Temperature [$^{\circ}\text{C}$]	Specific Heat [kJ/(kg K)]	Density [kg/m ³]
Universal Steel	T=20	0.14	T=20	0.425	7850 cst
	T=200	0.16	T=600	0.760	
	T=400	0.19	T=650	0.812	
	T=600	0.22	T=735	5.0	
	T=700	0.24	T=800	0.8	
			T=900	0.65	

Table 5: Thermophysical properties for the universal steel beam and column

The version 4 of FDS differs mainly from the earlier versions in its ability to model burning of charring fuels, like wood. The heat transfer and pyrolysis of charring materials are described using a one-dimensional model^{9, 10}. However, although it was tested in simple cases with reasonable good results, when it was used in the current simulations didn't seem to work satisfactorily. So a decision was taken to use the pyrolysis model for thermoplastic materials.

With thermoplastic materials it is assumed that fuel pyrolysis takes place at the surface, thus the heat required to vaporise fuel is extracted from the incoming energy flux. The burning rate, m'' , is given by an Arrhenius expression:

$$m'' = A\rho_s e^{\frac{-E}{RT}} \quad (6)$$

where, R , ρ_s , A , E , and T are the universal gas constant, the material density, a constant, the activation energy, and the temperature, respectively. Because A and E were not known, the burning rate was calculated by using two additional factors, namely the critical mass flux, m_{crit} , and the ignition temperature, T_{ign} . Then A and E were calculated in a way that the fuel burns at the m_{crit} rate when its surface reaches the T_{ign} temperature. The values used in the present study were $m_{\text{crit}} = 0.02 \text{ kg}/(\text{m}^2\text{s})$ and $T_{\text{ign}} = 350 \text{ }^\circ\text{C}$. The heat of vaporisation was taken equal to $H_{\text{vap}} = 500 \text{ kJ}/\text{kg}$. In order to prevent excess pyrolysis of fuel due to uncertainties, a maximum burning was prescribed, $m''_{\text{max}} = 0.1 \text{ kg}/(\text{m}^2\text{s})$; that limits the burning rate of the fuel to its measured maximum.

According to the ultimate analysis of the Western Hemlock softwood the number of carbon, oxygen, and hydrogen atoms in a fuel molecule are $x = 4.3$, $y = 5.8$, and $z = 2.6$, respectively. The "fuel" can now be written as $\text{C}_{4.3}\text{H}_{5.8}\text{O}_{2.6}$ with $M_f = 99$. The input parameters used to define the reaction (1) are $\nu_{\text{O}_2} = 4.4$, $\nu_{\text{CO}_2} = 4.2$, $\nu_{\text{H}_2\text{O}} = 2.9$, $y_s = 0.01$, and $\Delta H_{\text{O}_2} = 11020 \text{ kJ}/\text{kg}$.

The ignition for all the simulations achieved by defining an exponential function. The ignition of the wood cribs for Test 1 and 2 was to the rear row while in Test 7 all the wood cribs ignited simultaneously. All the surrounding materials assumed to be dry while the moisture of the wood cribs defined to be 9%. These values represent the claims that all the construction materials kept dry during the fire tests and that the wood was dried to moisture content of 8-10%. However, there were evidences that this was not 100% true for all the fire tests.

Two slightly different input file-cases were prepared for Test 1. The main differences in the second case are expressed with the following input data: $\Delta H_{\text{O}_2} = 12000 \text{ kJ}/\text{kg}$, $m_{\text{crit}} = 0.012 \text{ kg}/(\text{m}^2\text{s})$, while the suppression algorithm was deactivated.

Turbulence resolved with the large eddy simulation model choosing the default values. The default radiation model with the default values was also used. The only difference was for the Vicuclad panel for which the emissivity, the value of 0.7 was used.

All the solid materials considered as "thermally thick". When a solid material prescribed as thermally thick than the heat transfer equation is solved across the thickness of the material. However, the model includes a few important limitations. The first issue is that the code solves a one-dimensional version of the heat transfer equation, without the option to solve multi-layer materials. That means that the code only considers the thermal properties of the outermost material layer. For the backside of the material, it is assumed that the layer backs to an air gap at ambient temperature or that it backs up to an insulated material, which means there is no heat loss. As neither of these correspond to the real situation, a lot of attention should be paid for reasonable and reliable results. In the present simulations all the solid materials assumed to be "back insulated".

5 RESULTS AND DISCUSSION

A few of the results are presented below. The aim in this section was not to present the best correlated results, but rather the most representative. The results were chosen in a way to

identify the crucial and most important issues, and they represent the "whole general view" of the current study. We also refer to Test 1, modified Test 1, Test 2, and Test 7 as Case 1-1, Case 1-2, Case 2, and Case 7, respectively.

5.1 General comments

The grid size is the most important numerical parameter in the model, as it dictates the spatial and temporal accuracy of the discretised partial differential equations. The heat release rate is the most important physical parameter, as it is the source term in the energy equation. Property data, like the thermal conductivity, density, heat of vaporization, heat capacity, etc., ought to be assessed in terms of their influence on the heat release rate. In our case the heat release rate was not prescribed explicitly, but rather predicted by the model using the thermophysical properties of the fuel. The model output proved to be sensitive, sometimes to even minor changes in these properties.

As mentioned above the sensitivity of the radiation model was not examined, instead the default model with the defaults values was used. However, even with the simple radiation model in use, the radiation calculations cost about 50% of the CPU power and time. Another general observation was that errors of 100 % in heat flux, or even more, were caused by errors of 20 % in absolute temperature.

Unfortunately the charring pyrolysis model, introduced in the current version of the FDS software, could not be used in the present simulations. There was no clear evidence what the problem was; however, when it was tested in a small compartment, with a single wood crib as the fuel source, the results seemed to be reasonable good. It also seemed that when the fuel is wood, it is difficult to predict the growth rate and fire spread in a room without "tuning" carefully the pyrolysis rate coefficients. For real wood products, it is unlikely that all of the necessary properties can be obtained easily.

Although grid sensitivity and uncertain material properties make blind predictions of fire growth on real materials the model can still be used for at least a qualitative assessment of fire behaviour as long as the uncertainty in the flame spread rate is recognized.

5.2 Results

In all cases the pattern of fire growth was similar. After the ignition, the fire spread to adjacent lines of cribs and followed by a period of rapid development towards the crib line at the front. Once the fire was fully developed, the cribs from middle to the rear of the compartment were starved of oxygen with the result that combustion ceased. Burning continued near the opening and as the fuel was consumed, the fire progressed slowly back towards the rear. Although the cribs in Test 7 were ignited simultaneously, once the fire established itself the pattern of the behaviour displayed in the growing fires was repeated. Figure 9 shows the fire movement for Case 1-2.

Figure 10 compares the experimental measured data and the average-temperature calculated values above the crib line 2, 6, and 10, respectively. It may be seen that the calculated and measured ignition delay agree reasonably well in a sense. The calculated ignition delay was short but that was expected and it is the result of the pyrolysis model used.

The model used assumes that pyrolysis takes place at the wood surface, and that the fuel burns when it reaches the ignition temperature. In reality, pyrolysis takes place over a thin front, moving inside the material, and that gives the extra delay. As a result, in all cases presented here, the ignition delay was rather short and it was basically controlled by the thermal inertia of wood. However, the fire spread prediction was remarkably accurate. This can be easily seen from the left image (Figure 10), which refers to the rear of the compartment. The second temperature peak appears at exactly the same time, meaning that the flame-front was at the same position as it had been during the actual fire test. Also, both the peak temperature values are in excellent agreement with the measured ones. In a notable good agreement is also the temperature profile at the front crib line (right image). This is because the ventilation opening is there, and so well ventilation conditions exist. From this image, it can be also noticed the differences between Case 1-1 and Case 1-2 and how the properties of the fuel can influence the heat release rate, and of course the temperature, especially in well-ventilated conditions. The image in the middle represents the centre of the compartment. It can be seen that, although the first temperature peak was calculated with accuracy, afterwards the model could not predict the temperature profile with the same accuracy.

Actually, this was observed in all the cases; the middle sector of the compartment gives the least accurate results. From both, the left and middle images, it is obvious that the model failed to calculate the slope between the two temperature peaks with reasonably good accuracy. These are a multi-reason result and prove the complexity of the fire simulations. It is believed that the most important reason was the grid resolution. The grid was not fine enough to calculate accurately the gas concentrations and especially the oxygen (Figure 11). The lack of oxygen to the rear and middle section of the compartment causes the inaccurate estimation of the pyrolysis rate (that means also for the heat release rate); as a result the temperature distribution is questionable in that sector. Another reason is that FDS uses a mixture-fraction model without including the surface reactions. The lack of a surface oxidation model enhances (or at least helps) the uncertain results. Finally, we should keep in mind all the other significant assumptions made and mentioned in the previous sections.

Figure 12 shows a comparison for both the temperature values and radiation intensity on the wall lining at the centre of the compartment. It gives an idea of the error-scale in heat flux calculations when the absolute temperature is not predicted accurately.

Figure 13 gives the temperature distribution at two different positions (Figure 7). The inaccurate fast ignition is noticeable, however the absolute peak temperature values were predicted with very good accuracy. It is remarkable how the calculated values "follow" the measured data. It is an indication that the fire spread was predicted with excellent agreement. It is worth mentioning here that on the right image the model did not really predict the second temperature peak (actually there is a short decrease). This specific "behaviour" was investigated and is due to the mesh resolution. That is more obvious at later results.

Figure 14 gives the temperature predictions at the wall lining at three different positions. Again, the results "follow" the measured data with a qualitative good agreement, but with the same uncertainties mentioned above. Despite the fact that the error is rather high, we should keep in mind that the boundary layer was not resolved, the model uses a limited heat transfer model for solid obstacles, and also uses semi-empirical correlations. With these in mind the

results are considered surprisingly good. Finally, in Figure 15 we see the average temperatures above different crib lines. Again, the results are in good agreement, with the same uncertainties, but it is an additional confirmation that the fire spread was modelled accurately.

Two snap shots are given in Figure 16 for Test 7. It can be seen that after the first minutes the fire moved to the ventilation opening, while the flames extend to the outer space.

Figure 17 shows the results from a vertical thermocouple tree in the "group c" position (see Figure 3). The agreement is very good to all locations. In this figure, it is more obvious what we mentioned above. We can see that the model failed to predict the temperature peak and to mimic the measured results. As explained above this behaviour is due to the mesh used. However, in this case the error compared to the measured values is remarkable low.

Finally, Figure 18 presents another thermocouple tree that is close to the ventilation opening. Once again, it is noticeable that the model cannot predict the temperature rise in the same way as the measured data, however the present agreement can be even described as excellent. The fluctuated values, at probes 4 and 5, are because there is the position where the model predicted the layer height, but the mesh is not fine enough to resolve the area.

6 CONCLUSIONS

The FDS software was used to simulate three large-scale fire tests. A short description of the experimental concept is given followed by a brief discussion for the software used. Details about the problem set-up are also given. A few representative results are given and discussed. The main conclusions are given below:

- Mathematical modelling of fire is still young but a rapidly developing area of CFD. The complexity of the phenomenon involved makes it challenging
- FDS has been developed with emphasis to thermally driven flows and has been used successfully used for fire modelling. The models are designed and optimised for fire scenarios. It includes many options that are not yet available in commercial packages
- Despite the fact that charring model was not used, the calculated results were in good agreement with the experimental data in all cases
- In all cases the fire spread was in remarkably good agreement with the measured data
- The grid size proved to be the dominant parameter in the present study
- Heat release rate is the most important physical parameter. If it is not prescribed explicitly, than the input fuel properties should be carefully tested and "tuned"
- Finally, although grid sensitivity and uncertain material properties make blind predictions of fire spread and growth on real materials, the FDS can still be used for at least a qualitative assessment of fire behaviour as long as the uncertainty in the flame spread rate is recognized

7 ACKNOWLEDGEMENT

The present work was part of a Post-Doc Marie-Curie Fellowship (host fellowship contract No: MPMI-CT-1999-00047).

REFERENCES

- [1] P.J. DiNenno (editor), *SFPE Handbook of fire protection engineering*, National Fire Protection Association, 3rd edition, (2002).
- [2] D. Drysdale, *An introduction to fire dynamics*, John Wiley and Sons, 2nd edition, (2002).
- [3] J.G. Quintiere, *Principles of fire behaviour*, Delmar Publishers, (1998).
- [4] B.R. Kirby, D.E. Wainman, L.N. Tomlinson, T.R. Ray and B.N. Peacock, *Natural fires in large scale compartments*, A British Steel Technical, Fire Research Station Collaborative Report, British Steel Technical, Swinden Laboratories, UK, (1994).
- [5] G.M.E. Cooke, *Tests to determine the behaviour of fully developed natural fires in a large compartment*, BRE, UK, (1998).
- [6] K.B. McGrattan (editor). *Fire Dynamics Simulator (version 4) - Technical reference guide*, NIST Special Publication 1018, National Institute of Standards and Technology, (2004).
- [7] K.B. McGrattan and G.P. Forney. *Fire Dynamics Simulator (version 4) - User's guide*, NIST Special Publication 1019, National Institute of Standards and Technology, (2004).
- [8] R.G. Rehm and H.R. Baum. "The Equations of Motion for Thermally Driven, Buoyant Flows", *Journal of Research of the NBS (now NIST)*, **83**, 297-308 (1978).
- [9] A. Atreya, *Pyrolysis, Ignition and Fire Spread on Horizontal Surfaces of Wood*, NBS GCR 83-449, National Bureau of Standards (now NIST), (1983).
- [10] S.J. Ritchie, K.D. Steckler, A. Hamins, T.G. Cleary, J.C. Yang, and T. Kashiwagi, "The effect of sample size on the heat release rate of charring materials", *Fire Safety Science - Proceedings of the 5th International Symposium*, 177–188 (1997).

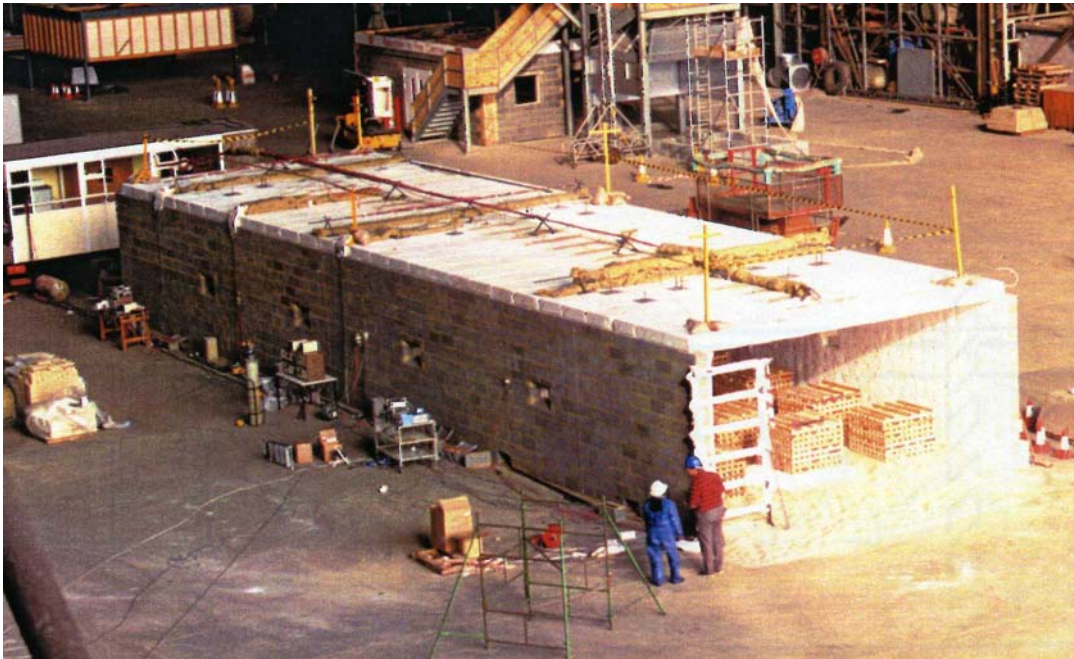


Figure 1: General view of the test compartment

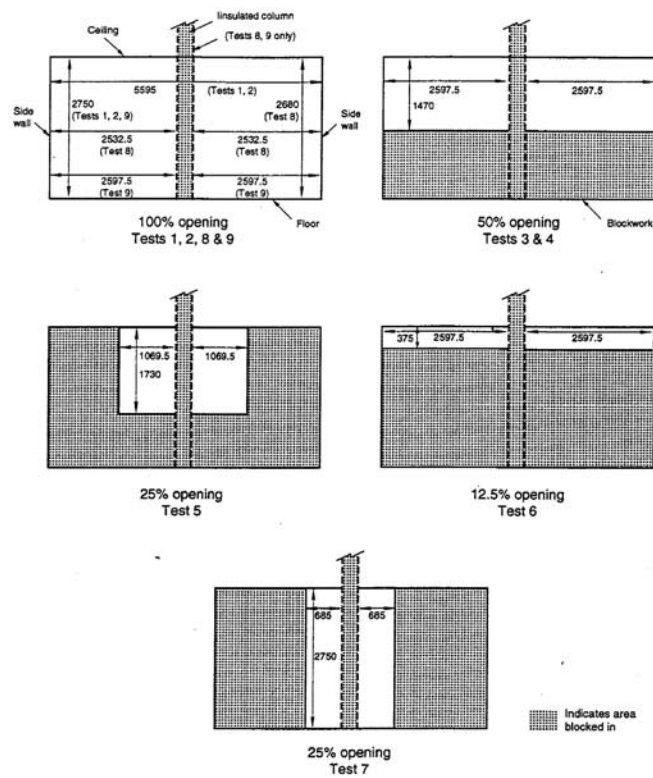


Figure 2: The ventilation openings

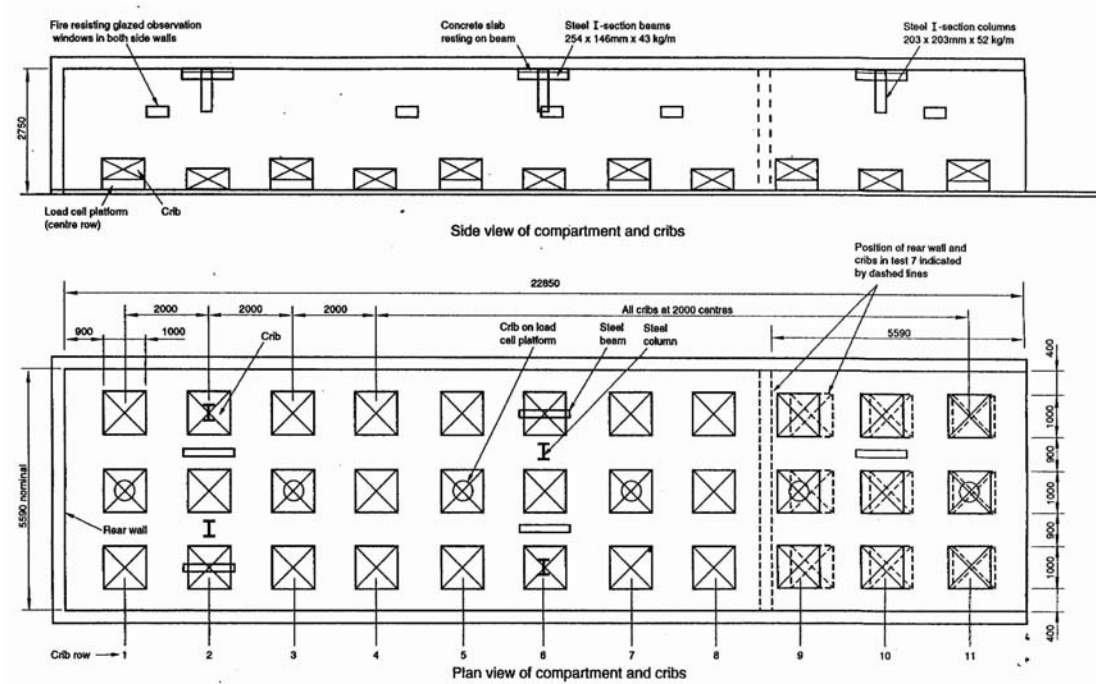


Figure 3: Compartment plan detailing the layout cribs



Figure 4: Construction of the wood cribs

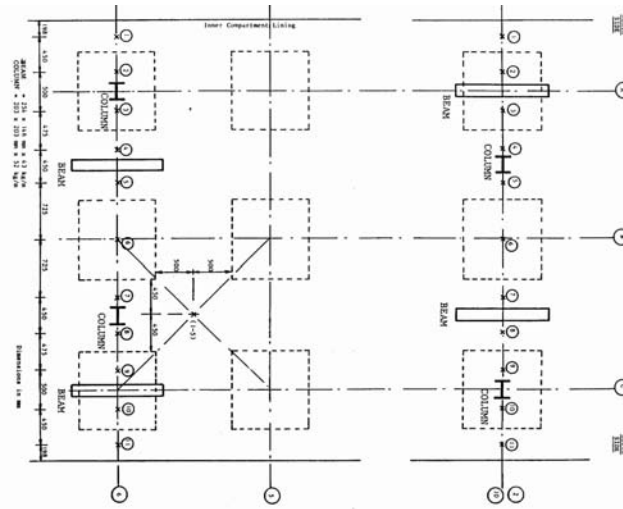


Figure 5: Plan detailing the position of the steel members and atmosphere thermocouples

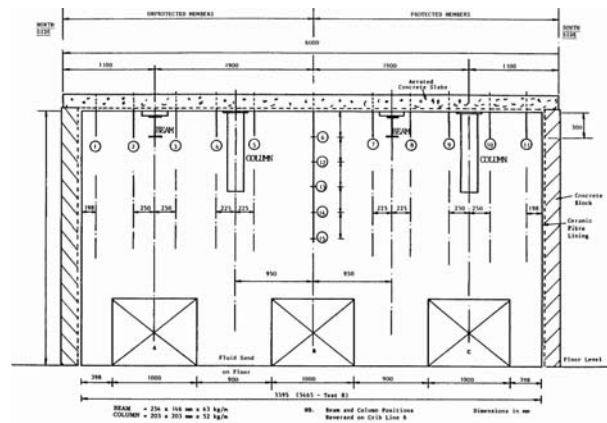


Figure 6: Plan detailing the position of the steel members and atmosphere thermocouples

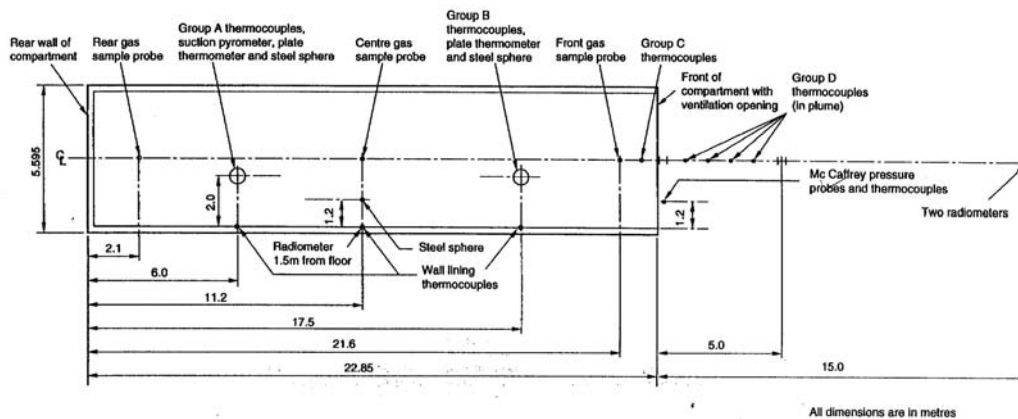


Figure 7: Plan view showing positions of instrumentation

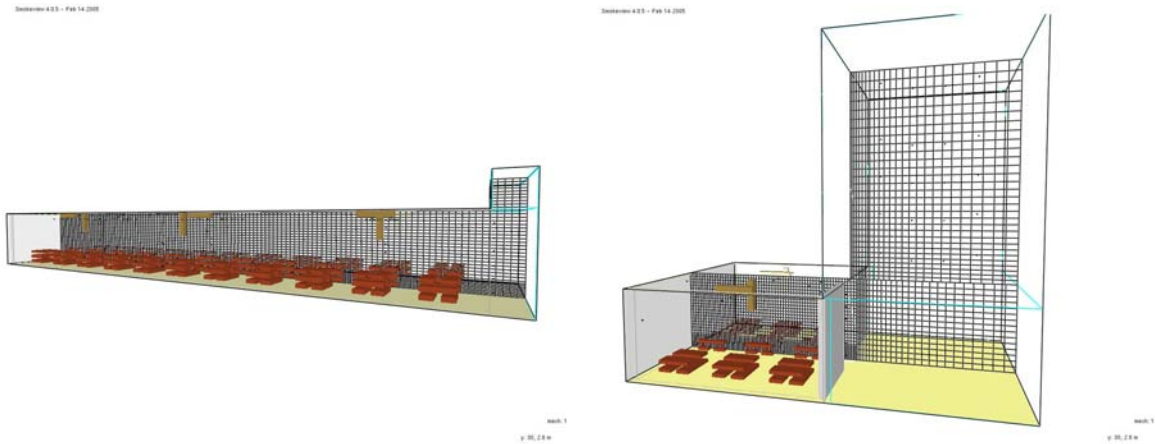


Figure 8: Grid and geometry used for Test 1 (left) and Test 7 (right)

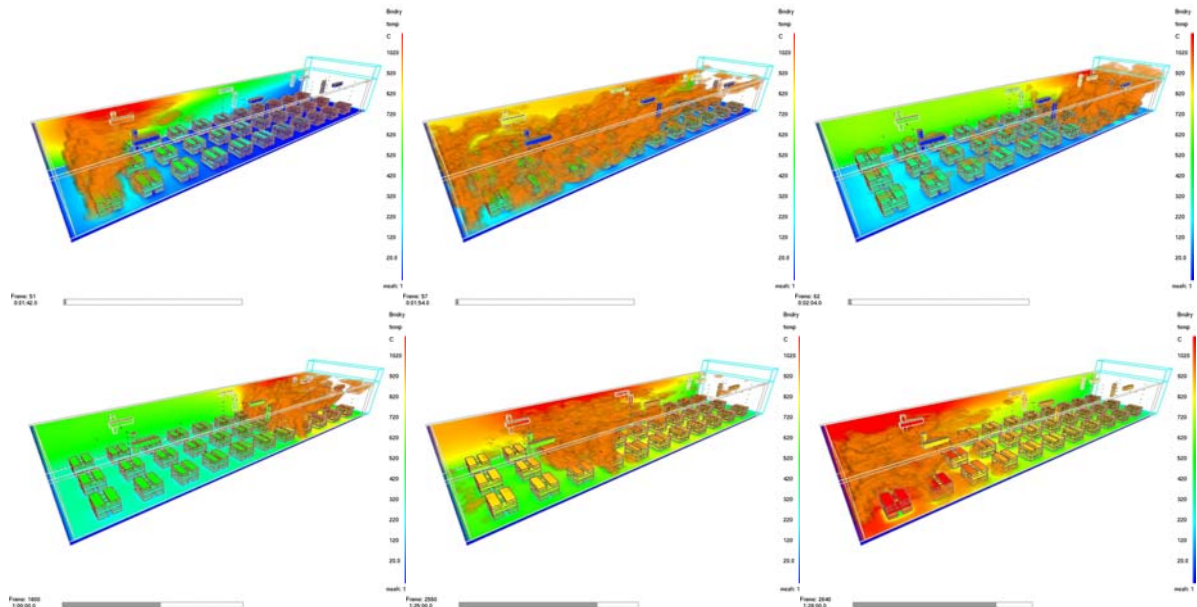


Figure 9: Fire spread and temperature distribution at the boundaries, Test 2

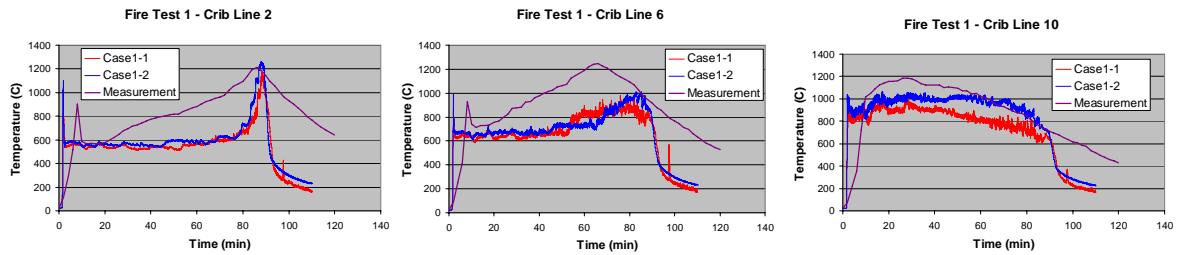


Figure 10: Mean temperature values and measurement data above crib line 2, 6, and 10, Test 1

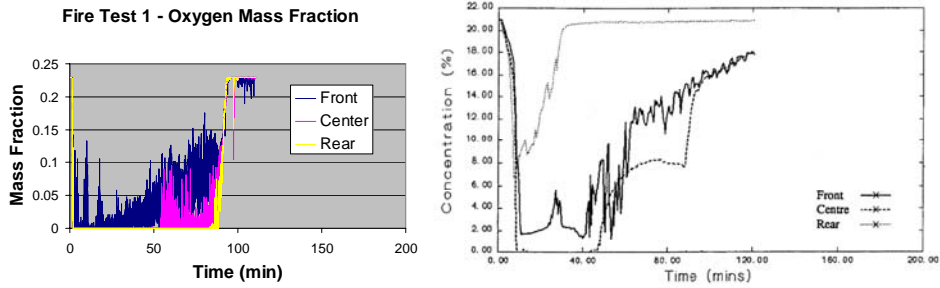


Figure 11: Mass fraction concentration of oxygen, Case 1-1

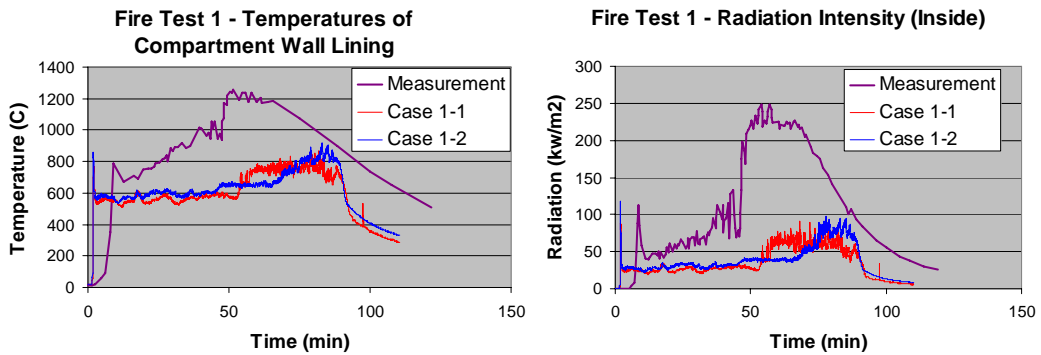


Figure 12: Wall temperatures (left) and radiation intensity (right) at the centre of the compartment, Test 1

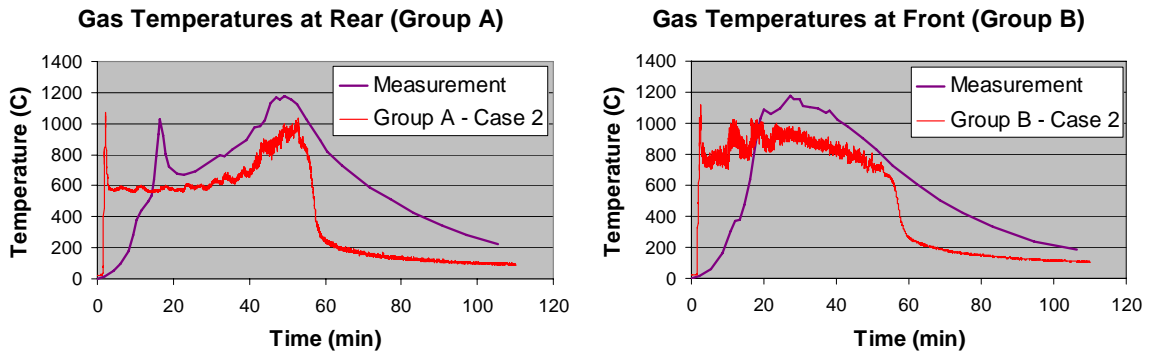


Figure 13: Gas temperatures at rear (left) and at front (right) of the compartment, Test 2

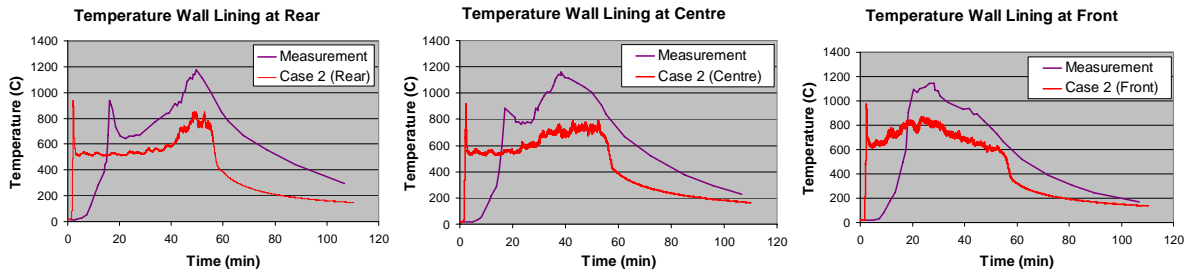


Figure 14: Temperatures of compartment wall lining, Test 2

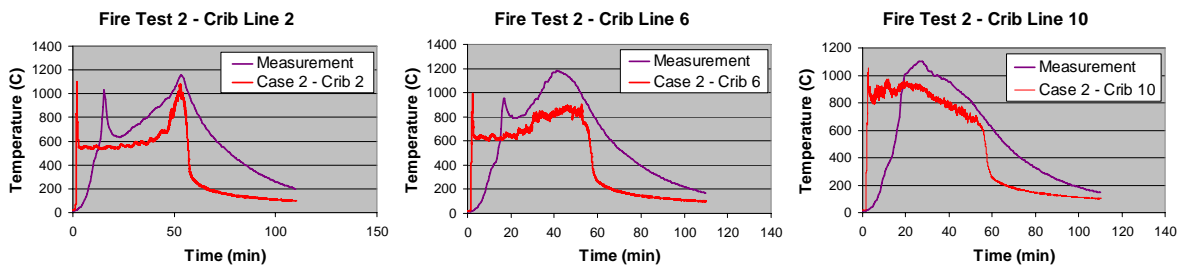


Figure 15: Mean temperatures values and measurement data above crib lines 2, 6, and 10, Test 2

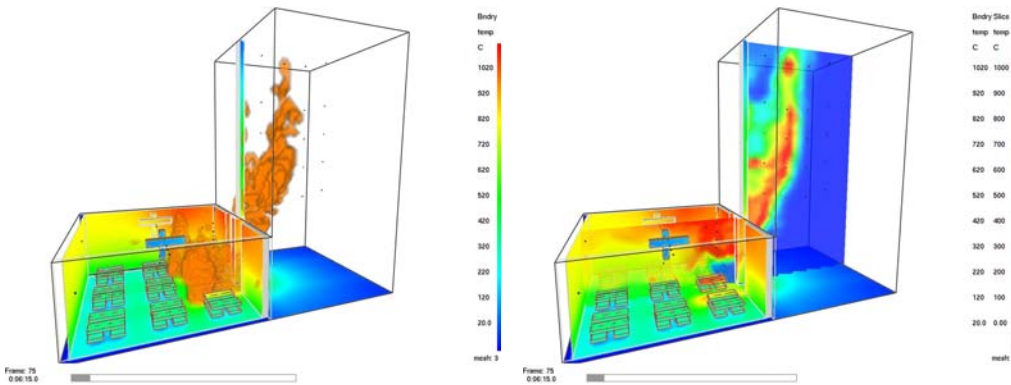


Figure 16: Snap shots , Test 7

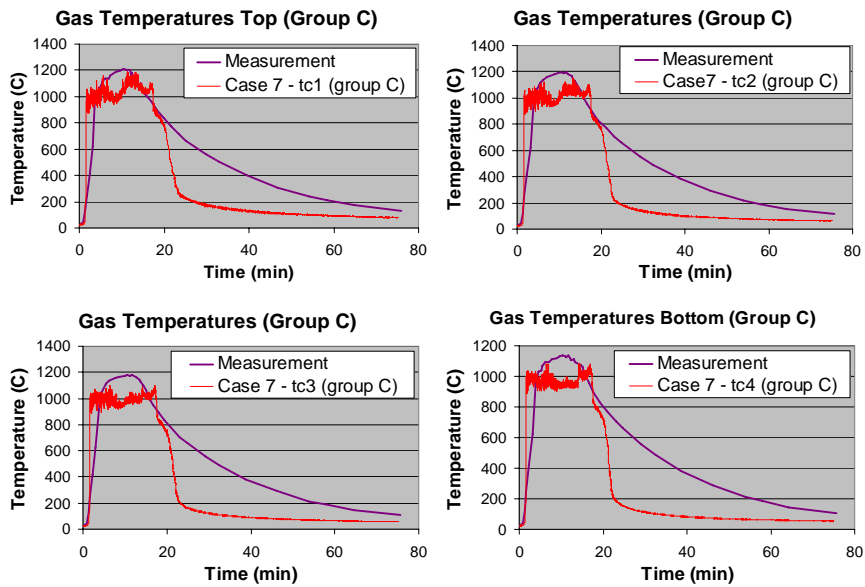


Figure 17: Gas temperatures measured by a thermocouple tree near front (group c), Test 7

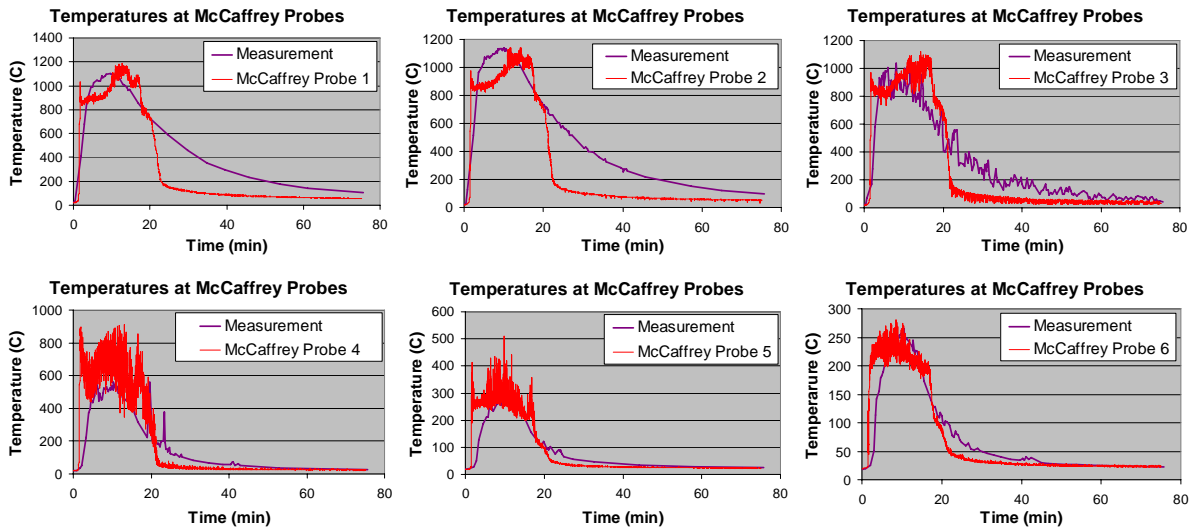


Figure 18: Gas temperatures at McCaffrey probe positions (Probe 1 refers to top and Probe 6 to bottom), Test 7